



**HAL**  
open science

## Evaluation of SFR Deformed Core Reactivity

M Gentili, B. Fontaine, G. Rimpault

► **To cite this version:**

M Gentili, B. Fontaine, G. Rimpault. Evaluation of SFR Deformed Core Reactivity. ICAPP 2015 - International Congress on Advances in Nuclear Power Plants, May 2015, Nice, France. cea-02933399

**HAL Id: cea-02933399**

**<https://cea.hal.science/cea-02933399>**

Submitted on 8 Sep 2020

**HAL** is a multi-disciplinary open access archive for the deposit and dissemination of scientific research documents, whether they are published or not. The documents may come from teaching and research institutions in France or abroad, or from public or private research centers.

L'archive ouverte pluridisciplinaire **HAL**, est destinée au dépôt et à la diffusion de documents scientifiques de niveau recherche, publiés ou non, émanant des établissements d'enseignement et de recherche français ou étrangers, des laboratoires publics ou privés.

## Evaluation of SFR Deformed Core Reactivity

M.Gentili<sup>1,2</sup>, B.Fontaine<sup>1</sup>, G. Rimpault<sup>1</sup>

<sup>1</sup>CEA, DEN, DER, Cadarache 13108 Saint Paul Lez Durance, France

<sup>2</sup>Aix Marseille Université, 13284, Marseille, France

\*e-mail to: [michele.gentili@cea.fr](mailto:michele.gentili@cea.fr)

**Abstract** – *In the framework of the development of the Sodium Fast Reactor technology (SFR) the analysis of all possible scenarios leading to perturbation of nominal operating condition is exploited. Among these scenarios attention is being paid on reactivity modification due to core assemblies bowing and deformation, and to lattice readjustments consequent to earthquakes. A computational scheme based on the spatial projection method fulfilling a good compromise between the accuracy of stochastic codes and the quick runtime of deterministic codes has been developed and used to determine the reactivity changes issued from core lattice deformations and irregularities. The calculation of reactivity changes induced by core deformation is achieved by modifying the isotopic concentrations of assemblies concerned by displacements, by projecting the deformed lattice geometry on that corresponding to regular reference case. This methodology was validated by comparison with stochastic codes, and good agreements between the results achieved and those obtained by the Monte Carlo code TRIPOLI4 are observed. The deterministic code available at CEA for fast reactors, i.e. ERANOS/PARIS, has been used to solve neutron transport equation in a full 3D core representation and to calculate the reactivity changes due to core flowering and compaction. In this work, such a method has been used to determine the maximal positive/negative reactivity insertion corresponding to a postulated mechanical energy supplied to an SFR core, as much as the lattice deformation causing it. The results presented in this paper, represent a first step in the assessment of a favourable calculation scheme that can be easily scaled-up to large-sized core and used for the future application in core design and safety analysis.*

### I. INTRODUCTION

Fast reactor designs are currently being revisited aiming at having a consolidated safety dossier. In that frame, studying any perturbation of nominal operating condition is mandatory<sup>1</sup>.

Among different initiators, particular attention is being paid on reactivity insertion due to core assemblies bowing and deformation and induced lattice readjustments as consequence of events such as earthquakes<sup>2</sup>.

In the case of a SFR core, significant reactivity increases consequently to core compaction may arise. In fact because of the gaps between the assemblies the most reactive configuration differs from normal operation conditions.

Even if stochastic codes based on Monte Carlo method allow a precise evaluation of core reactivity in its deformed configuration, the long computation time and the significant needs of memory needs they are characterized by, do not make such a method compatible for core design

iteration process, which require many core deformation situations, or for seismic response simulations. On the other hands deterministic codes guarantee reduced costs in terms of simulations run time, preventing although stochastic codes precision to be achieved.

In this work, a first approach in the estimation of an SFR core lattice deformation maximizing positive and negative reactivity insertion, as a function of the mechanical energy provided to the reactor core is presented. An *a-priori* evaluation of  $\Delta\rho$  has been fulfilled starting from individual assemblies displacement reactivity worth, issued from ERANOS<sup>3</sup> perturbation module coupled with a deterministic computation scheme based on mesh projection method.

A precise description of assemblies mechanical interaction is not the purpose of this work, which is mainly focused on proposing a first neutronic approach for an *a-priori* estimation of deformed core reactivity.

In the following sections a description of the deterministic computation scheme developed for reactivity

changes estimation is reported, as much as preliminary results in deformed core reactivity evaluation for the French SFR prototype Phénix<sup>4</sup>.

## II. LOCAL LATTICE DEFORMATIONS IMPACT ON SFR CORE REACTIVITY

A simplified model<sup>5</sup> has been proposed by the authors with the purpose of identifying the impact of different neutronic phenomena affecting reactivity in case of local deformation of the hexagonal assembly lattice for a SFR. In this section a brief summary of the model is proposed and attention will be pay on core reactivity changes issued from individual assembly shifting, as a function of the assembly nature and position into the core, as well as its dependence from displacement direction and intensity.

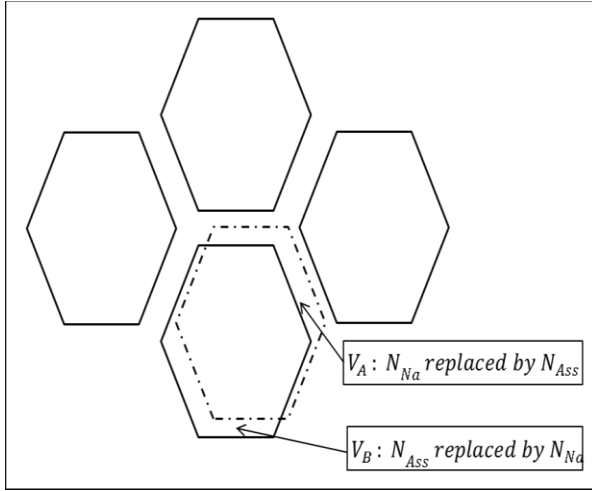


Fig. 1. Assembly displacement 2D representation and local changes in sodium ( $N_{Na}$ ) and in assembly isotopes ( $N_{Ass,i}$ ) concentration.

For sake of simplicity different assumptions have been made in developing the model:

- *One energy group;*
- *Diffusion approximation<sup>6</sup>;*
- *First order perturbation theory;*
- *Microscopic cross sections not affected by the perturbation.*

For the purpose of this work, the assumptions made guarantee the dependence of individual assembly reactivity worth by its displacement or deformation to be determined without lack of precision. Nevertheless such hypothesis can be easily relaxed in order to determine precisely the nature of different contributions to  $\Delta\rho$  as functions of the lattice deformation considered<sup>5,7</sup>.

An axial discretization  $h$  is introduced to take into account more complex deformation as bowing or bending characterized by deformation axial gradient different from zero.

Referring to Fig. 1. an assembly displacement involves local changes and redistribution of isotopic concentration and so of macroscopic cross sections  $\Sigma$ . In particular, since first order perturbation theory<sup>8</sup> is used ( $\Phi_{pert} \cong \Phi_{unPert}$ ) and isotopic microscopic cross sections are retained to be not affected by lattice deformations, changes in macroscopic cross sections of isotope  $i$  for the reaction  $j$  will be:

$$\delta\Sigma_{i,j} = \delta N_i \sigma_{i,j} \quad (1)$$

Again, it follows that the perturbation will affect just volumes  $V_{A,h}$  and  $V_{B,h}$ , implying perturbation integrals to be null outside these spatial domains.

In order to determine the reactivity change induced by an assembly displacement in the direction  $\vec{u}_{d,h}$ , a small deformation approximation is introduced. In particular we consider that for an assembly whose center projection on 2D plane is  $P(x, y)$ , the perturbation is negligible ( $N_{i,h} \gg \delta N_{i,h}$ ) and localized in the regions  $P_A$  and  $P_B$  around the displaced assembly. Furthermore In a 1D representation along the displacement axis, the distance between  $P_A$  and  $P_B$  will be:

$$\|P_A - P_B\|_h = s \vec{u}_{d,h} \quad (2)$$

where  $s$  is the size of the assembly.

With a short-cut in notation we can define:

$$\begin{aligned} \delta N_{ih}(P) &= \delta N_{i,h} \delta(P - P_{Ass}) \\ \int_V \delta N_{ih}(P) \Phi(P) &= \delta N_{i,h} \Phi(P - P_{Ass}) \end{aligned} \quad (3)$$

where  $P_{Ass}$  represents the assembly center and, because of the assumptions made, the neutronic flux results to be just a function of space.

By combining equations (1), (2), (3) and first order perturbation theory formulation, and considering a first-order expansion for neutronic flux  $\Phi$  and its adjoint  $\Phi^*$ , the reactivity variation induced by a fuel assembly centered in  $P(x, y)$  will be<sup>5</sup>:

$$\Delta\rho_P = -\sum_h K_{P,h} \langle \nabla(\Phi\Phi^*)_P | \vec{u}_{d,h} \rangle \quad (4)$$

In order to put in evidence the relation between  $\Delta\rho$ , assembly position and lattice deformation, the dependence from changes in isotopic concentration is resumed in term  $K_{P,h}$ , function of displacement length  $|\vec{d}|$

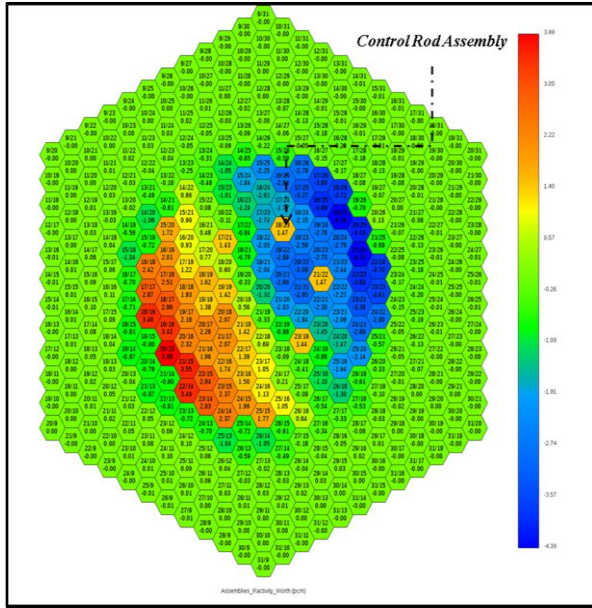


Fig. 2. Assembly reactivity worth (pcm) for  $\vec{u}_d = \left[ \frac{\sqrt{3}}{2}; 1 \right]$  (Phénix core application).

According to diffusion approximation, the term  $\nabla(\phi\phi^*)_P$  represents the derivative of the product of spatial direct flux and adjoint flux in radial direction  $\vec{u}_P = \frac{P-P_0}{\|P-P_0\|}$  where  $P_0 = (x_0, y_0)$  represents the core center. It follows that the directions which maximize and minimize the individual assembly reactivity contribution will correspond to centripetal and centrifugal directions respectively:

$$\max_{\Delta\rho_P} \vec{u}_d = -\vec{u}_P \quad \min_{\Delta\rho_P} \vec{u}_d = \vec{u}_P \quad (5)$$

Exceptions will arise for control rods assemblies or those in correspondence of fertile/reflector interfaces, where  $\max(\vec{u}_d)$  and  $\min(\vec{u}_d)$  mainly depend mostly by changes in concentration and by neighboring assemblies nature.

Moreover, because no perturbation in microscopic cross section is considered, and since  $\Phi_{pert} \cong \Phi_{unPert}$ , we can estimate (as first a approximation) deformed core reactivity starting from individual assemblies reactivity contributions:

$$\Delta\rho \cong \sum_P \Delta\rho_P \quad (6)$$

Fig. 3. reports a comparison between diffusion calculation (DIF3D), transport  $S_N$  calculation (SNATCH) and an estimation of  $\Delta\rho$  using (6).

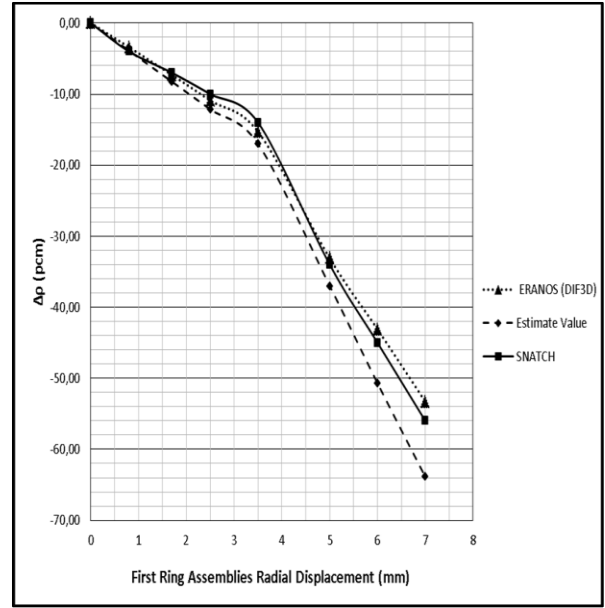


Fig. 3. Reactivity changes induced by the displacement of the two innermost fuel assemblies rings evaluated with spatial projection method.

The more the assemblies displacements are small the more such assumptions, and consequently (6) results to be verified: as reported in Fig. 3. Deviancy from calculated results in fact, increases as core deformation involves a larger number of assemblies and larger displacements, remaining less than 15% both for diffusion and transport calculations.

### III. ASSEMBLIES REACTIVITY WORTH EVALUATION

In order to simulate core lattice deformation and to determinate the assemblies reactivity worth, a computational scheme based on spatial projection method and deterministic codes has been used<sup>5</sup>.

The perturbations in the reactor lattice are simulated by modifying the isotopic concentrations of those cells which correspond to displaced or deformed assemblies. The perturbed concentrations are calculated by projecting the deformed lattice geometry on the regular one.

Neutron flux and reactivity evaluation issue from a two-step approach necessary to reduce the number of variables required to describe precisely core heterogeneities and geometric complexity, providing first an estimation cross sections resonances and self-shielding phenomena, and then the resolution of both diffusion or transport equation starting from macroscopic cross sections previously evaluated.

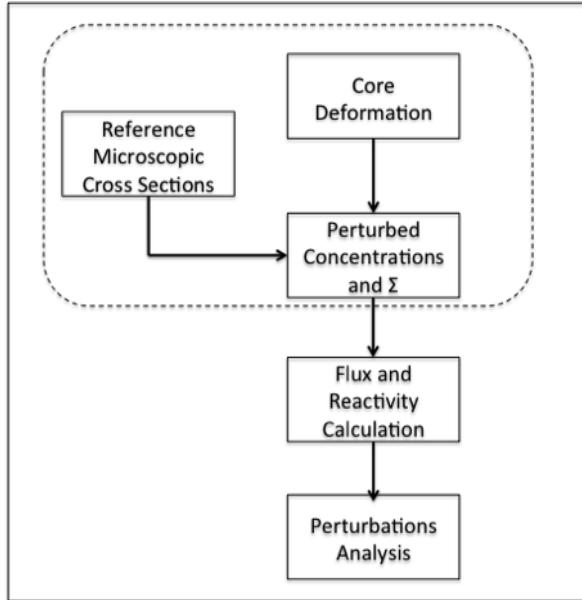


Fig. 4. Calculation scheme representation.

As represented in Fig. 4., once microscopic cross sections for each core region are calculated, changes in macroscopic cross sections are evaluated according to (1), starting from variations in isotopic concentrations issued from a core deformation, provided as an input in terms of assemblies displacements.

For this work the self-shielded microscopic isotopic cross sections for 33 energy groups have been calculated with ECCO<sup>9</sup> cell code for fast reactors, referring to the JEFF3.1<sup>10</sup> neutronic data library.

The ERANOS perturbations module based on DIF3D<sup>3</sup> solver has been used to evaluate changes in  $\Delta\rho$  consequent to single assembly shifting in several directions and in correspondence of different core regions and configurations.

Confirmations of (4) have been achieved identifying the inward/outward direction to be the one maximizing/minimizing  $\Delta\rho_P$ .

The individual contributions of Phénix assemblies in inward direction, corresponding to 1 mm displacement are reported in Fig. 5. For the sake of simplicity, because of the core symmetrical geometry and assembly nature, a sixth-core representation is reported.

Referring to the Phénix core the deformations and displacements which mostly affect core reactivity involve assemblies concerning interface regions, as fissile/fertile interface and fertile/reflector ones.

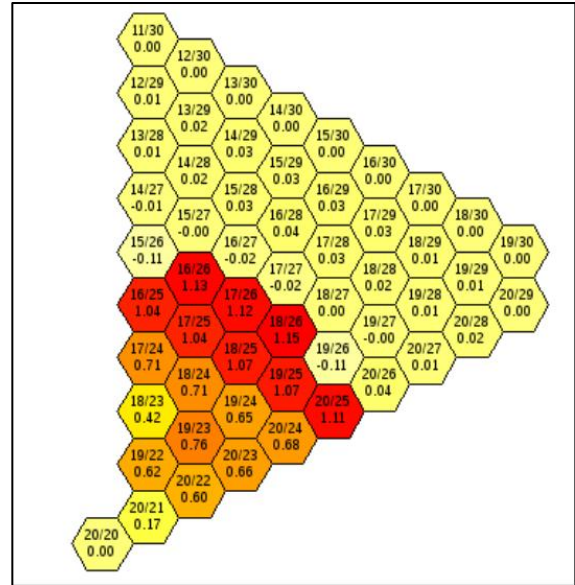


Fig. 5. Phénix core Assembly Reactivity Worth (pcm) for  $\max_{\Delta\rho_P} \bar{u}_d$  and  $|\bar{u}_d| = 1 \text{ mm}$  (Phénix core application).

#### IV. CORE DEFORMATION REACTIVITY ESTIMATION

In this section an iterative method based on individual assemblies reactivity worth is proposed, in order to provide an *a-priori* estimation of reactivity insertion consequent to a core lattice deformation.

In particular, such a method as been applied with the purpose of determining the assemblies displacements field which maximizes/minimizes  $\Delta\rho$  in correspondence of the mechanical energy  $E$  supplied to the core.

As a first approach, this work does not deal with a precise description of assemblies mechanical interaction and its relationship with the energy supplied to the reactor core. Its purpose is to show instead how the most reactive core deformation can be estimated just starting from individual assembly reactivity worth.

In this work no assemblies bowing or bending is considered. To take into account these phenomena, ameliorations of the method will be object of future works.

For these reason several assumptions concerning the problem mechanical formulation have been taken into account:

- No friction interactions between assemblies have been considered;
- The sodium flow does not provide any mechanical resistance to assemblies displacement;
- Hence: the total energy supplied to the core concerns assemblies displacements. Just assemblies potential energy is considered.

- All core assemblies have the same mechanical properties, expressed in terms of  $k [N/mm]$ .

As stated in chapter III, because of Phénix<sup>4</sup> symmetrical core configuration, the evaluation of assemblies reactivity worth has been fulfilled in correspondence of a sixth part of the whole core, and for 24 displacement directions.

A first order approximation has been then used to calculate  $\Delta\rho_p$  as a function of assembly displacement module  $|\vec{u}_{d,p}|$ . In fact, because of the dependence of isotopic concentrations changes and  $K_p$  (4) from the displacement length, it is possible to write:

$$\Delta\rho_p \cong \alpha |\vec{u}_{d,p}| - \beta |\vec{u}_{d,p}|^2 \quad \alpha \gg \beta \quad (7)$$

Identifying  $\Delta\rho_{p,1}(\vartheta_{d,p})$  as the reactivity variation induced by an assembly shift of  $|\vec{u}_{d,p}| = 1 \text{ mm}$  in the direction  $\vartheta_d$  it follows:

$$\Delta\rho_p(|\vec{u}_{d,p}|, \vartheta_{d,p}) = |\vec{u}_{d,p}| \Delta\rho_{p,1}(\vartheta_d) \quad (8)$$

According to the assumptions previously made, all the energy supplied to the core concern the assemblies shifting from their original position:

$$E = \frac{1}{2} k \sum_p |\vec{u}_{d,p}|^2 \quad (9)$$

Checks on the distance between assemblies are carried at each iteration, in order to let the geometrical configuration that guarantees the maximal reactivity insertion, to be a physical lattice deformation. Then:

$$\Delta\rho_{Max} = \max_E \sum_p |\vec{u}_{d,p}| \Delta\rho_{p,1}(\vartheta_{d,p}) \quad (10)$$

Since the reactivity worth of each assembly has been evaluated just for 24 displacement directions, the direction maximizing  $\Delta\rho_{p,1}$  is considered. Equation (9) becomes therefore:

$$\Delta\rho_{Max} = \max_E \sum_p |\vec{u}_{d,p}| \Delta\rho_{p,1}(\vartheta_{MAX,p}) \quad (11)$$

In particular, the most reactive core deformation results to be characterized by a displacements field which is directly proportional to assemblies individual contributions:  $|\vec{u}_{d,p}|_{MAX} = \gamma \Delta\rho_{p,1}(\vartheta_{MAX,p})$ .

It follows that:

$$\Delta\rho_{Max} = \gamma \sum_p [\Delta\rho_{p,1}(\vartheta_{MAX,p})]^2 \quad (12)$$

where the constant  $\gamma$  is a function of the energy considered.

The same procedure is used to determine the minimal reactivity insertion corresponding to the energy  $E$ .

The impact of approximations (8) and (11) on estimation of deformed core reactivity will be discussed later in this paper.

#### IV.A Maximal Positive Reactivity Insertion

In this section a comparisons between the estimated maximal reactivity insertion and the results issued from deterministic calculations is reported.

Such an analysis has been fulfilled taken into account two main parameters:

- The minimal distance allowed between hexagonal wrappers of fuel assemblies.
- The mechanical properties of fuel assemblies expressed by term  $k$ .

In fact, since in the model no assemblies pad have been considered, their presence can be approximatively taken into account by considering different values of sodium gap between the assemblies. Furthermore suggestions about the impact of pad deformation resistance to  $\Delta\rho$  have been achieved by using different values of  $k$ .

The first scenario considered deals with the absence of assembly pads.

In particular the sodium gap ( $\Delta l = 3.5 \text{ mm}$ ) and mechanical resistance ( $k = 1000 [N/mm]$ ) considered in this scenario refer to Phénix core properties in its nominal state<sup>4</sup>.

The deformation considered involves fuel and fertile assemblies, while no reflector assemblies displacements are considered.

For the sake of simplicity hereunder a comparison is reported for deformations for which  $\Delta\rho \leq 1\%$  ( $1\% \cong 350 \text{ pcm}$ ).

To be specific, in core design activities, this values (1%) is retained to be the maximal reactivity that can be inserted into the core in case of its deformation<sup>11</sup>.

As displayed in Fig. 6, the *a-priori* approach overestimate the deterministic results, issued from reactivity calculation in correspondence of the deformed geometry.

As mentioned before, such a deviancy from calculations arises from assumptions (8) and (11). Reduced deviancies could be achieved with a finer description of  $\Delta\rho_{p,1}(|\vec{u}_{d,p}|, \vartheta_{d,p})$ , involving a larger number of displacement directions, as much as the introduction of the second order term in  $\Delta\rho_p$  dependence from the displacement length.

The results achieved have then been compared with those issued from hypothetical core deformation scenarios:

- Core compaction starting from outer rings assemblies (*Outer*);
- Core compaction starting from inner rings assemblies (*Inner*);
- Homogeneous core compaction (*Homogenous*).

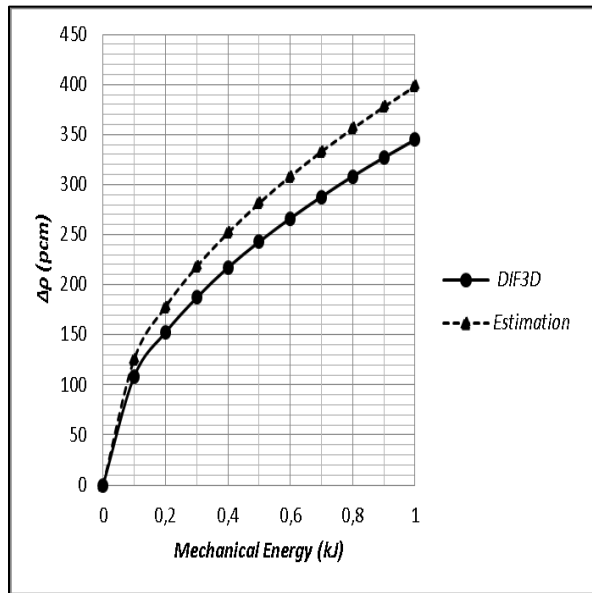


Fig. 6. Comparison between maximal reactivity insertions estimated and calculated with ERANOS DIF3D solver.

Even for these scenarios, the reactivity changes induced by deformation have been estimated starting from each assembly contributions by using (6).

In particular, the homogeneous core compaction is usually considered as the reference deformation in the perspective of the respect of safety issues in core design activities.

As reported in Fig. 7. in the range of energies considered, a core deformation concerning assemblies compaction starting from inner rings and progressively involving outer assemblies (*Inner*), leads to values of  $\Delta\rho$  broadly smaller than the one involving outer assemblies (*Outer*). As reported in Fig. 5 in fact, inner assemblies are characterized both by smaller values of  $\Delta\rho_{P,1}$  than those located in fifth and sixth ring.

Again, the reactivity insertion consequent to a *homogenous* core compaction is slightly inferior to that the *Most Reactive* one, issued from (11). By comparing these two kinds of deformation it follows that, referring to the assumptions made, a 1\$ insertion is attained at lower energies for the *Most Reactive* configuration ( $\cong 0.1$  kJ lower).

Furthermore it is possible to define:

$$\delta\rho = \Delta\rho_{MR}(E_{1\$,MR}) - \Delta\rho_{Hom}(E_{1\$,MR}) \quad (13)$$

as the deviancy between the two models in correspondence of the energy at which the *Most Reactive* configuration (MR) is concerned by a 1\$ reactivity insertion. In this case  $\delta\rho \cong 5\%$ .

All the scenarios converge to the same values of  $\Delta\rho = 3.73$  \$ when a full core compaction ( $\Delta l \rightarrow 0$  mm) is considered ( $E = 12.225$  kJ).

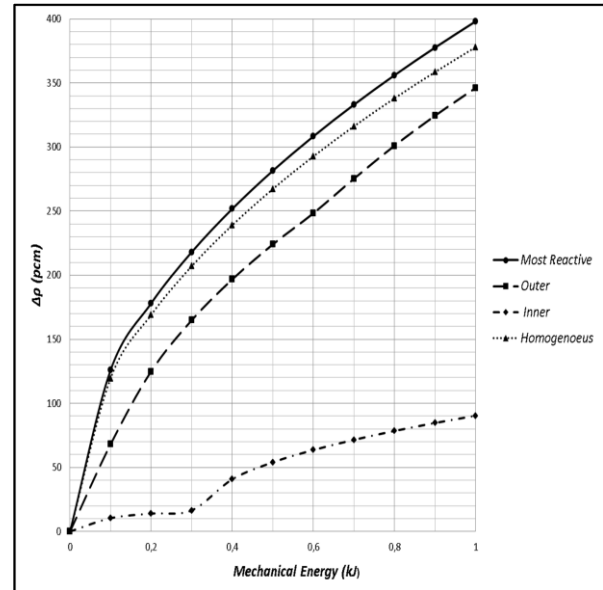


Fig. 7. Maximal reactivity insertion issued from different deformations scenarios.

As previously stated, the presence of assembly pads has been taken into account through different values of the sodium gap length  $\Delta l$ . For this analysis just the most reactive configuration has been considered (*Most Reactive*).

Since the trends of  $\Delta\rho_{Max}$  overlap for the pad sizes considered, just the maximal reactivity insertion corresponding to the most compact core configuration ( $\Delta l = 0$ ), as much as the mechanical energy supplied to attain  $\Delta\rho = 1$  \$, is reported in Tab. 1.

Smaller the assembly gaps smaller the assemblies displacements and therefore smaller values of  $\Delta\rho_{\Delta l=0}$ . Conversely,  $E_{1\$}$  increases slightly with the presence of pads and a 1\$ insertion is never reached for  $\Delta l \rightarrow 0$ .

The impact of the presence of pads on  $\delta\rho$  is negligible.

TABLE I

Maximal Core Compaction Reactivity Insertion

Gap Between Assembly Pads (mm)	$E_{1\$}$ (kJ)	$E_{\Delta l=0}$ (kJ)	$\Delta\rho_{\Delta l=0}$ (pcm)
0.5	-	0.25	186.5
1.5	0.88	2.25	569.3
2.5	0.77	6.25	941.5
3.5	0.75	12.23	1300.8

In its reference configuration, Phénix core fuel assemblies are equipped with pads that guarantee core compactness at nominal operating conditions. In order to determine the pads deformations and the values of  $\vec{u}_{d,p}$  that would lead to core compactness, a complete mechanical investigation should be accomplished. As previously reminded, such an analysis goes beyond the aim of this paper. However, looking at Tab. 1. it is possible to predict how this core configuration would be characterized by smaller values of  $\Delta\rho_{Max}$  and therefore by a safer neutronic behavior.

Furthermore, because of the high amount of energy required to gain the pads elastic resistance, higher values of  $E$  would be required to attain a core deformation that entails  $\Delta\rho = 1\$$ .

Different values of the constant  $k$  have been taken into account with the purpose of predict, in a preliminary way, the impact of assemblies mechanical properties on  $\Delta\rho(E)$ .

The effects of both a higher and a lower assemblies resistance to shifting and displacement have been analyzed by increasing and reducing the  $k$  values.

For the sake of simplicity, in Fig. 8 the trends of  $\Delta\rho(E)$  is displayed for the reference case ( $k = 1000 [N/mm]$ ) and for core configuration into which the mechanical constant is reduced/increased by a factor 2.

As suggested by (9), because of the direct proportionality relation between  $k$  and  $|\vec{u}_{d,p}(E)|$ , for configurations foreseeing an increased resistance to deformation (increased pads and lattice stiffness), a larger amount of energy need to be supplied to the core in order to insert 1\$ of reactivity.

The opposite trend is observed lower values of  $k$ .

As n case of assemblies equipped pads, no remarkable variations of  $\delta\rho$  arise.

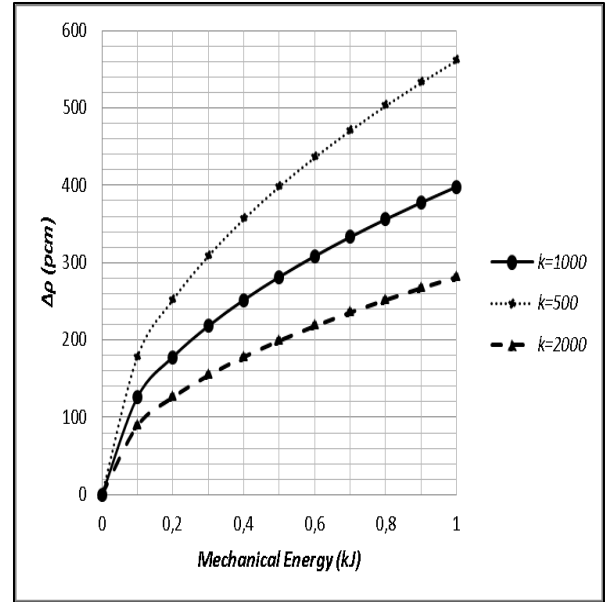


Fig. 8. Maximal reactivity insertion in correspondence of different values of the  $k$ . No assemblies pads are considered.

Moreover, the mechanical energy necessary to attain full core compaction ( $E_{\Delta l=0}$ ) and a prompt-critical configuration is reported in Tab. 2.

TABLE II

Maximal Core Compaction Energy as function of  $k$

$k [N/mm]$	$E_{1\$}$ (kJ)	$E_{\Delta l=0}$ (kJ)
500	0.39	6.05
1000	0.77	12.23
2000	1.55	24.45

The same tendencies are observed in dealing with pad-equipped assemblies.

#### IV.B Maximal Negative Reactivity Insertion

The same method has been then applied to determine the maximal negative reactivity insertion ( $\Delta\rho_{Min}$ ) inserted into the core because of a lattice deformation. As suggested by (5) such a deformation is characterized by assemblies shifting towards outward directions.

In this section just a comparison between  $\Delta\rho_{Min}$  estimated with the method proposed into this paper and with a homogeneous deformation is proposed. The impact of pad-equipped assemblies and of lattice stiffness has been observed to be comparable to the one evaluated in §IV.A

Conversely from core compaction, a deformation issued from a homogenous core expansion largely differs from the one which maximizes  $\Delta\rho_{Min}$ .

As previously expressed in (12), the maximal negative reactivity insertion can be written as:

$$\Delta\rho_{Min} = \xi \sum_P [\Delta\rho_{P,1}(\vartheta_{MIN,P})]^2 \quad (14)$$

As stated by (14) in fact, the deformation will affect first the assemblies with larger  $\Delta\rho_{P,1}(\vartheta_{MIN,P})$ , so the outer core regions.

On the other hand, in case of homogeneous core expansion, referring to the same amount of energy supplied to the core, the deformation will affect mostly the inner regions of the core, characterized by lower values of  $\Delta\rho_{P,1}(\vartheta_{MIN,P})$ .

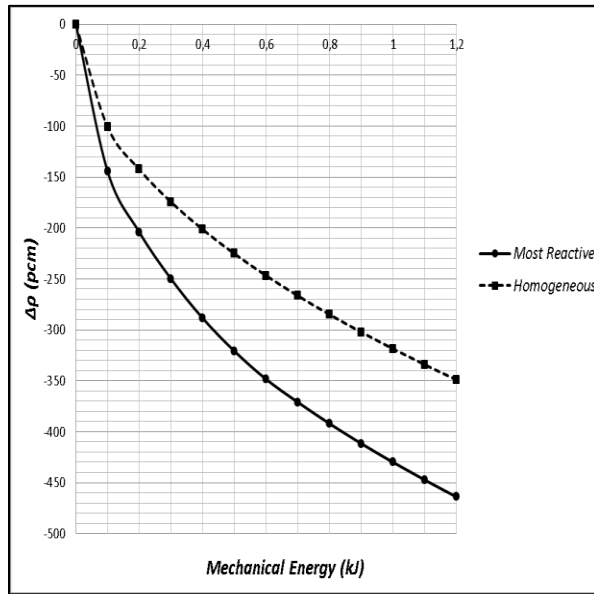


Fig. 9. Maximal negative reactivity insertion. No assemblies pads are considered.

For this reasons the *Most Reactive* deformation is characterized by broadly inferior values of  $E_{1\$}$  ( $\cong 0.6 kJ$  lower than the *Homogeneous* case), and in respect to core compaction, higher deviancy between the two models is observed for  $E_{1\$,MR}$  ( $\delta\rho \cong 28\%$ ).

## V. CONCLUSIONS

The evaluation of core neutronic behavior consequent to core assemblies bowing and deformation or lattice modifications consequent to earthquakes or impulsive loads, is one of the main challenge fast reactor core designer are faced to.

A precise evaluation of the deformed core reactivity is in fact necessary in order to respect properly reactor safety

requirements and constraints the core design activities are subject to.

Since deterministic scenarios of core deformations are very challenging (seismic local time history, core deformation origin, gap size distribution), some assumptions have to be made in design phases to represent core deformations, with indicative conservative level.

In particular, a homogeneous core geometry modification (both in the sense of core compaction and expansion), is considered usually as the reference deformation taken into account for safety evaluation.

In this work, a simple method has been developed and tested in order to determine the maximal positive and negative reactivity insertion issued from core deformation induced by a postulated mechanical energy supplied to an SFR core. Conversely to the homogeneous case, no *a-priori* assumptions concerning the possible deformations scenario have been made.

A preliminary analysis based on perturbation theory has been fulfilled in order to determine the relation between core assemblies and the reactivity insertion consequent to their displacement. In particular, for small lattice perturbations, the possibility of estimating changes in reactivity of the whole core starting from local contributions is put in evidence.

The deviancy of estimated results from those achieved by DIF3D direct calculation increases as larger assemblies displacement fields are considered. Our method overestimates the reactivity perturbations guaranteeing, from a safety point of view, a conservative estimation of deformed SFR core neutronic behavior. Anyway, discrepancies remain lower than 15 %.

Several hypotheses concerning the mechanical interaction between the assemblies have been done.

Because of these assumptions, the analysis fulfilled in this work cannot provide a precise and complete evaluation of the maximal reactivity insertion attainable as a function of the energy supplied to the core, but it represents a first important step in this direction.

In fact, results put in evidence how homogenous geometry modifications may not be representative of the worst core deformation scenario. Moreover such a scenario, characterized by a displacements field which results directly proportional to individual contributions can be determined simply by starting from local contributions, avoiding any hypothesis on lattice modifications to be done.

The possibility of take into account core different assemblies features, as for instance pad size have been exploited in §IV.A.

In order to improve the method performances, a deeper analysis in core mechanics is necessary, as much as a complete evaluation of  $\Delta\rho_P$  allowing the relaxation the assumption (8) and the description of assemblies bowing or bending.

However, several information on deformed core behavior can be achieved with the method object of this work. In particular, progresses from a safety point of view have been attained because of the possibility of determining the most reactive core configuration simply starting from its neutronic description.

The methodology proposed in this paper represents a first step in the assessment of a favorable calculation scheme that can be easily scaled-up to large-sized core.

## REFERENCES

1. GIF DOE-GIF, 2002. "A Technology Roadmap for Generation IV Nuclear Energy Systems." Technical Report GIF2002200, GIF.
2. T. J. MORAN, "Core restraint contributions to radial expansion reactivity", ASME/ANS Nuclear Power Conference, Philadelphia, USA, (1986).
3. G. RIMPAULT et al. "The ERANOS code data system for fast reactor neutronic analyses", Proc. of The Physics of Fuel Cycles and Advanced Nuclear Systems (PHYSOR 2002), Seoul, Korea (2002).
4. J.M. CHAUMONT, D. Goux, L. Martin, "Some safety related characteristics of Phénix, a 250 MWe fast reactor - 1989 and 1990 negative reactivity trip investigations", ANP'92: International Conference on Design and Safety of Advanced Nuclear Power Plants, Tokyo (Japan), October (1992), pp. 25-29.
5. M. GENTILI, B. Fontaine, G. Rimpault, "Deformed Core reactivity Evaluation with Mesh Projection Based Method", Nuclear Technology, NT14-123, (accepted, to be published).
6. A.E WALTAR et al., "Fast Spectrum Reactors", Springer, 2012.
7. M. REED, K Smith., B Forget., "The 'virtual density' principle of neutronics: Toward rapid computation of reactivity effects in practical core distortion scenarios", Proceedings of the 2013 International Conference on Mathematics and Computational Methods Applied to Nuclear Science and Engineering - M and C 2013.
8. M. L. WILLIAMS, "Perturbation Theory for Nuclear Reactor Analysis" CRC Handbook of Nuclear Reactors Calculations, Vol. III, CRC Press, Inc., Boca Raton, Florida, 1986.
9. G. RIMPAULT. "Physics documentation of ERANOS and the ECCO cell code", Technical report, Rapport Technique RT/SPRC/LEPh 97-001, 1997.
10. A. KONING et al, "The JEFF-3.1 Nuclear Data Library" Nuclear Energy Agency Data Bank, OECD, JEFF Report 21, NEA N° 6190, (2006).
11. P. SCIORA, et al., "Low void effect core design applied on 2400 MWth SFR reactor" - Proceedings of ICAPP 2011, Nice, France, May 2-5, 2011.
12. B. FONTAINE et al., "Description and preliminary results of PHÉNIX core flowering test", Nuclear Engineering and Design, volume (241), pp. 4143-4151.